

Hybrid multi power sources PEMFC/battery/supercapacitor real time setup energy conversion system

Riad Moualek¹, Nacereddine Benamrouche¹, Nabil Benyahia², Amar Bousbaine³

¹LATAGE Laboratory, Mouloud Mammeri University, Tizi-Ouzou, Algeria

²Department Electrical Engineering, ESME Sudria School of Engineers, Paris, France

³College of Science and Engineering, University of Derby, Derby, United Kingdom

Article Info

Article history:

Received Nov 16, 2022

Revised Mar 19, 2023

Accepted Mar 29, 2023

Keywords:

Battery
DC-DC converters
Energy management
Fuel cells
Supercapacitor

ABSTRACT

This paper presents an energy management system with multiple sources. The proton exchange membrane fuel cell as the main power drive source is used when needed. However, because of its slow rate it is combined with a battery and supercapacitor racks as secondary sources. The proposed energy conversion system ensures the energy demand of an electric vehicle. The storage system, which includes a battery and a supercapacitor, provides a high level of performance in both autonomy and availability of power. The battery as a primary storage source, feeds the whole system during cruise processes. At needs and during accelerations phases, the supercapacitor, takes over and reacts to supply the load. This topology keeps the fuel cell disconnected from the bus supply, until the battery reaches a critical voltage level. At this time, the fuel cell kicks in and charges the battery rack. The entire system was initially tested using MATLAB/Simulink environment and the outcome findings were subsequently analyzed. The simulated results have been corroborated experimentally using a test rig based on dSPACE real time interface. Experimental results indicate that the suggested approach is capable of meeting the electric vehicle energy requirements.

This is an open access article under the [CC BY-SA](https://creativecommons.org/licenses/by-sa/4.0/) license.



Corresponding Author:

Riad Moualek
LATAGE Laboratory, Mouloud Mammeri University
Tizi-Ouzou, BP 17 RP, 15000, Tizi-Ouzou, Algeria
Email: rmoualekfr@yahoo.fr

1. INTRODUCTION

Atmospheric CO₂ concentrations have risen by over 40% due to human activities, as a result of particularly the burning of carbon based fuels, since the beginning of the industrial revolution, and more than half of this increase has occurred since 1970 [1]. According to data released by the energy information administration, transportation of both people and goods constitutes around a quarter of the world's energy consumption, with light-duty vehicles for passenger transportation being the primary contributor to this energy usage [1]. In 2012, the combined consumption of motor gasoline (including ethanol blends) and diesel (including biodiesel blends) made up 77% of the total energy consumed in the transportation sector [2]. Accounting for around 23% of energy-related CO₂ emissions (6.7 Gt CO₂) in 2010, the transportation sector generated 7.0 Gt CO₂ eq of direct greenhouse gas emissions (including non-CO₂ gases). One potential solution to this issue lies in transitioning to electro mobility, which involves replacing gasoline and diesel vehicles with electric vehicles (EVs) [3], [4].

Climate change causing environmental issues were placed among the top five global risks expected to happen in the next decade, according to the 2020 global risks perception survey conducted by the world economic forum [5], [6]. The transportation sector is a crucial pillar of a nation's economy, exerting a

significant influence on the direction and rate of economic development [7]. Moreover, in many countries, the transport industry has a notable impact on energy usage and related carbon dioxide emissions. The concentration of CO₂ in the atmosphere has risen by over 40% since pre-industrial times, with more than half of this increase happening after 1970. Additionally, methane has increased by more than 150% and nitrous oxide has increased by approximately 20% [8]. The warming of the Earth is influenced by the increase in all three gases, but CO₂ has the most significant impact [6].

According to a report by the intergovernmental panel on climate change (IPCC), the demand for global energy is projected to increase significantly by the end of the century, from 10 TW to almost 46 TW by 2100. Fossil fuels are expected to continue dominating the energy sector until 2030, accounting for approximately 83% of the overall increase in energy demand between 2004 and 2030 [9], [10]. By 2030, the international energy agency (IEA) predicts that there will be an increase of 14.3 Gt CO₂ compared to the 2004 level [10]. Increasing levels of anthropogenic CO₂ will lead to a rise of almost 6 °C in the average global temperature by 2100, which would result in thermal expansion of the oceans and melting of the polar ice caps. These changes would cause floods and storms. According to the international energy agency (IEA), road transport is responsible for 17% of global greenhouse gas (GHG) emissions, and this carbon flow has increased by 2-3% annually over the past two decades [11], [12].

Adopting electric vehicles (EVs) and hybrid electric vehicles (HEVs) can help mitigate CO₂ emissions. EVs are a crucial component in achieving global climate change goals and are a prominent feature in the mitigation strategies aimed at limiting the rise in temperature to below 1.5 °C, as outlined in the Paris Agreement. Until 2030, the impact of electric vehicles (EVs) on reducing CO₂ emissions will be relatively low, even with ambitious plans for their adoption, as indicated by a recent paper [13], [14]. Despite this, evidence suggests that after 2030, the adoption of electric vehicles (EVs) in all scenarios will lead to a significant increase in the number of EVs on the road and a cumulative reduction in CO₂ emissions [15], [16]. To switch to a low carbon emissions passenger transport fleet in the mid-term and meet near-term CO₂ emission mitigation targets, cities, regions, and countries must establish a specific policy framework for electric vehicles (EVs) and consider additional alternatives such as modal shift and incentivized telecommuting.

One of key solution is the move to a pure electric vehicle (PEV) [6], [9], [17] and the fuel cell hybrid electric vehicle (FCHEV), is among the most promising for the cleanest mode of transport of the future [12], [18]. The EVs offers a high energy density where two concepts are applied. The first approach involves powering the vehicle using its own batteries and charging them via known stationary charging terminals [10], [19]. However, this method is often criticized since the energy for these charging stations often comes from non-renewable sources such as fossil fuels. The second approach is less harmful and offers vehicles greater autonomy and efficiency by using fuel cells (FCs) as the primary power source, which is linked to an energy storage system (ESS) and has a reduced carbon impact [13], [20], [21]. This paper focuses on FCs type based on the proton exchange membrane fuel cell (PEMFC) electric vehicle power management system. The proposed prototype of the PEMFC electric vehicle system comprises a fuel cell, a battery, and a supercapacitor. The system is simulated using MATLAB Simulink, an industrial-based software, and management approach. The system's performance is tested using a real-time setup and the dSPACE 1103 interactive interface.

This paper is organized as follows: i) Section 2 deals with the system's configuration and description; ii) Section 3 presents a detailed model of the used PEM fuel cell; iii) Section 4 discusses the emulator of the fuel cell used and the experimental results; and iv) Section 5 is dedicated for the validation. Interests are calculated. The experimental results of the real time hardware set-up are given and discussed the control strategies using buck-boost converters to manage the energy flow to and from the supercapacitor rack along with the simulation and experimental results is shown. the whole system of the energy management protocol (EMSP) is verified. Section 6, concludes the works and discusses the outcomes for the research undertaken.

2. SYSTEM DESCRIPTION

Figure 1 depicts the suggested scheme of the PEMFC electric vehicle. It includes a primary source represented by a PEMFC, which provides the whole system's energy. The dc bus voltage is controlled through a boost DC-DC converter using a proportional integral derivative control technique (PID). A battery rack closely linked to the dc bus voltage, provides the load with power during the high peak demands using power management protocol. The super capacitor rack also connected to the bus voltage through a buck-boost power converter. With respect to self-reliance and power availability, this type of hybrid storage system provides excellent performance [21]. In this topology, a heuristic energy management has been considered. The slow transient response of the fuel cell must be taken into account to avoid its premature damage [22]. An unbalanced management protocol will affect not only the fuel cell but also the battery life time leading to an inefficient power management system [22], [23].

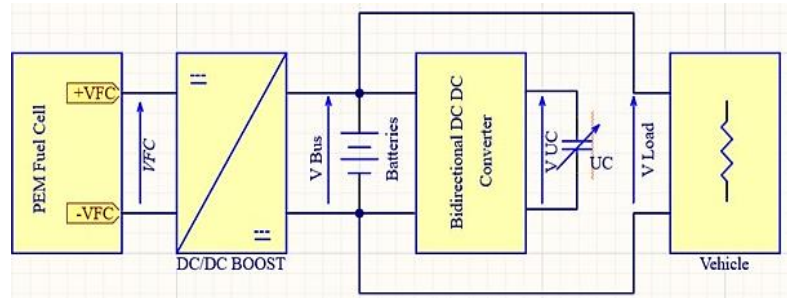


Figure 1. PEMFC based PEV topology

3. SYSTEM MODELING

3.1. PEM fuel cell modeling

In this paper, a 500 W proton exchange fuel cell model is emulated using an electronic circuit in order to prototype an electric vehicle. However, the fuel cell is known to present a slow dynamic rate [24]–[26]. This issue is taken care off during the peak power periods using the power energy management and will also consequently improve the efficiency of the system [27], [28]. During the last decades, several management methods were developed such as fuzzy rule control [29], [30], deterministic rule control [31] or global optimization [32], bio inspired optimization methods [33] and model predictive control management [34]. Our study proposes an optimal heuristic method for power management of fuel cell hybrid electric vehicle system, using a fuel cell emulator built around a power voltage source controlled using a buck converter for a fast dynamic response. Owing to the inherent characteristics of the fuel cell and its requirements, the net voltage generated by the cell is lower than its internal voltage. This can be attributed to multiple voltage drops that occur during the operation of the PEMFC, caused by the natural functioning of the fuel cell and the chemical processes taking place inside it. The fuel cell has the advantage of being clean [35] and its principle of operation is based on the conversion of chemical energy contained in hydrogen covalent bound to electrical energy as shown by the equations below. In the anode (oxidation):



in the cathode (Reduction):



the global chemical reaction becomes:



the chemical energy produced from the fuel cell can be computed from the variation between products and reactants Gibbs free energy ΔG_f [21].

$$\Delta G_f = g_f(Product) - g_f(React) = g_f(H_2O) - g_f(H_2) - g_f(O_2) \quad (4)$$

In (5) shows that the Gibbs free energy varies with both temperature and pressure reactants, where ΔG_{0f} is the change in Gibbs free energy at standard pressure of 1 bar.

$$\Delta G_f = \Delta G_{0f} - RT_{fc} \log \left(\frac{P_{H_2} P_{O_2}^{0.5}}{P_{H_2O}} \right) \quad (5)$$

If the process is reversible, all chemical energy is converted into electricity. So, for each mole of Hydrogen, two moles of electrons are produced. The total electrical work given by (6) is equal to the Gibbs free energy released [21]. Note that the value is negative which means that the energy is released.

$$Electrical\ Work\ Done = \Delta G_f = -2FE_{Nernst} \quad (6)$$

Where F and E are respectively the faraday constant ($F = 96485$ C), and the open circuit fuel cell voltage called Nernst voltage for a reversible system. In our case (hydrogen fuel cell) at $25^\circ C$, $\Delta G_f = -237.2$ KJ and $E = 1.229$ V for each cell. Using a thermodynamic expression, in the standard state entropy variation, in (7) is expended and yields [36], [37]:

$$E = 1.229 - 0.85 \cdot 10^{-4} (T_{fc} - T_0) + 4.3085 \cdot 10^{-5} T_{fc} [\ln(P_{H_2}) + 0.5 \ln(P_{O_2})] \quad (7)$$

where the absolute temperature $T_0 = 298.5^\circ K$ is expressed in Kelvin and pressure in atm. But in a real case the process is far from being totally reversible. Indeed, some losses appear and a fraction of the chemical energy is shifted to heat, then fuel cell voltage V_{cell} for each cell, is given by (8).

$$V_{cell} = E_{Nernst} - V_{act} - V_{ohm} - V_{conc} \quad (8)$$

After subtracting the whole losses whose expressions are given in (9), (10) and (11) equations, the final voltage fuel cell V_{fc} relation in (12).

$$V_{act} = \frac{RT}{\alpha z F} \ln\left(\frac{i_{fc}}{I_0}\right) \quad (9)$$

$$V_{ohm} = i_{fc} R_{ohm} \quad (10)$$

$$V_{conc} = \frac{RT}{\alpha z F} \ln\left(\frac{i_{Cs}}{C_b}\right) \quad (11)$$

$$V_{fc} = n_{fc} \cdot V_{cell} = n_{fc} (E_{Nernst} - V_{act} - V_{ohm} - V_{conc}) \quad (12)$$

Where: V_{act} : Activation voltage losses due to Hydrogen activation delayed time; V_{ohm} : Ohmic losses due to fuel cell making up materials; V_{conc} : Concentration losses due to the H_2 concentration level during crucial current requirement; n_{fc} : Number of cells; V_{cell} : Cell voltage; E_{Nernst} : Thermodynamic potential of the cell. P_{H_2}, P_{O_2} : Hydrogen and Oxygen partial pressures; and T_{fc} : The cell temperature.

The PEMFC characteristic hence depends on the gaseous flow and its depletion at the level of these electrodes. In case of a sudden load current change, an electrical transient occurs, resulting in a significant voltage drop. The magnitude of this voltage drop depends on various factors such as the gas and air accessibility at the electrodes, the speed of the chemical process responsible for electron production, and the materials used to construct the cell. The transient process ends once the throttle pressure is readjusted.

3.2. Battery modeling

In this paper a standard battery model provided by MATLAB/Simulink, is used to simulate the whole system. however, normalized equations are given to identify and perform the studied energy storage system (ESS). As known, the battery is an electrical device that converts the chemical energy stored in the covalent bonds, into electricity, producing one or more electrons for each bound, whatever the types of battery or electrolyte used. Considering a lead-acid battery, the global charge-discharge reaction is given by (13).



The easiest way to describe the general battery behavior is its voltage expression given in (14), and according to the equivalent electric circuit Figure 2.

$$V_{bat} = V_0 - i_{bat} R_{int} \quad (14)$$

As mentioned in [38], the battery state of charge (SOC) must be taken into account to perform accuracy behavior. Therefore, to achieve this aim, we include the SOC parameter as a state variable by introducing in the electric circuit Figure 3, a serial variable resistor such as (15):

$$R_{VR} = \frac{K}{SOC} \quad (15)$$

where the SOC variation allows us to get a battery voltage in the range. The global equation is then given as (16).

$$V_{bat} = V_0 - \left(R_{int} + \frac{K}{SOC}\right) i_{bat} \quad (16)$$

3.3. Supercapacitor modeling

As a high efficiency electrical energy storage component, and offering a high-power density with a high cycling capability, the supercapacitor model under extreme conditions of use, must describe accurately the voltage behavior and the energy flows during charge and discharge processes. Yet, and taking into

account some assumptions, considering for example the temperature as constant, supercapacitors are usually modelled using a simple RC circuit as depicted in Figure 4.

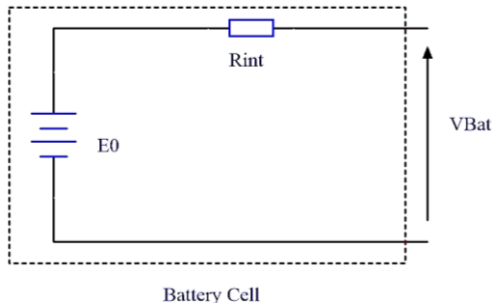


Figure 2. Battery equivalent electric circuit

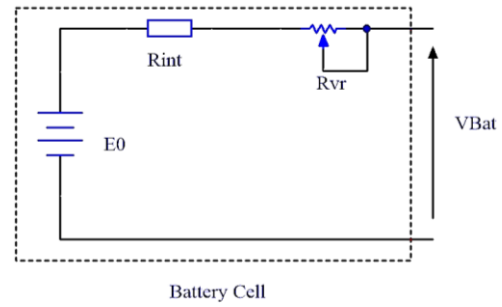


Figure 3. Battery equivalent electric circuit considering SOC parameter

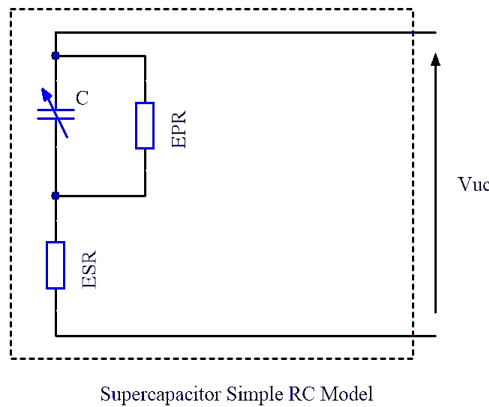


Figure 4. Supercapacitor electric equivalent circuit

Where *ESR* is the equivalent serial resistor, which is very small for simulating the heat losses. *EPR* is an equivalent parallel resistor used to simulate self-discharge leakage losses, and its value is relatively high. Meanwhile, *C* stands for a perfect capacitor. The mathematical model resulting from this includes various variables, such as capacity attributes, resistance attributes, lifespan attributes, leakage rate, and self-discharging. Among them, capacity and resistance have direct impact on the defined model. The relation (17) as follow defines the intrinsic capacity.

$$\Delta V = \frac{1}{C} \Delta t \tag{17}$$

Applying the relation expressed in (17), the supercapacitor working voltages, must be considered to be in range of $[V_{min}, V_{max}]$ and considering for each instant, in (18) is defined and verified.

$$V_{t1} = V_{t0} - \Delta V = V_{t0} - \frac{1}{C} \Delta t \tag{18}$$

Where, the supercapacitor voltage drops during t_0 and t_1 time laps. The SOC parameter is therefore defined using instant supercapacitor voltage V_{inst} and its working bounds as (19).

$$SOC = \frac{V_{inst} - V_{min}}{V_{max} - V_{min}} \tag{19}$$

The energy spent during the same time laps and between the two bounds is expressed in (20).

$$E = \frac{1}{C} (V_{max}^2 - V_{min}^2) \tag{20}$$

4. PEMFC BASED PEV SIMULATION RESULTS

Figure 5 displays the MATLAB/Simulink block diagram developed for testing the suggested approach, using the power system toolbox. The system main source is the PEM fuel cell, which, controlled accordingly, while the battery and supercapacitor function as backup power sources. During testing, the electric vehicle is exposed to a variable power load scenario, while the energy management system is designed to distribute the power demand of the PEM fuel cell electric vehicle across the entire system. The load comprises the electric vehicle and the storage battery model during the charging of the battery. The simulation results shown in Figure 6, illustrates that the proposed controlled power management and conversion system can meet the power load demand.

In Figure 6(a), the bus voltage remains constant at around 85V due to the PID regulator which controls the output of the converter despite the variation of the PEM fuel cell output voltage, V_{fc} . This is oscillating between 35 V and 40 V as shown in Figure 6(b). Figure 6(c) shows the balancing during a complete cycle. There are four curves, the first noted P_{BUS} represents the power profile of the load voltage. P_{Bat} curve shows the power provided by the battery, which is shouldered by the super capacitor reacting faster, as shown by P_{sc} curve. The power delivered by the fuel cell is depicted by P_{fc} curve; however, its dynamic is slower than the battery and the supercapacitor response. As expected, the secondary source consisting of the battery and supercapacitor racks reacts efficiently according to the control algorithm. While the fuel cell reacts as primary source and supplies the load with most of the power it needs. Through these results, we note that P_{BUS} is in all times the sum of the three powers sources and fulfill the power demand of the EV.

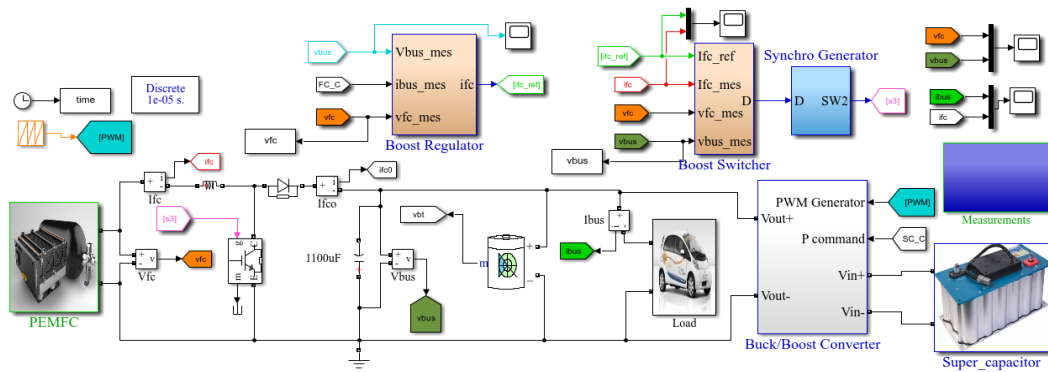


Figure 5. PEMFC based PEV simulation synoptic diagram

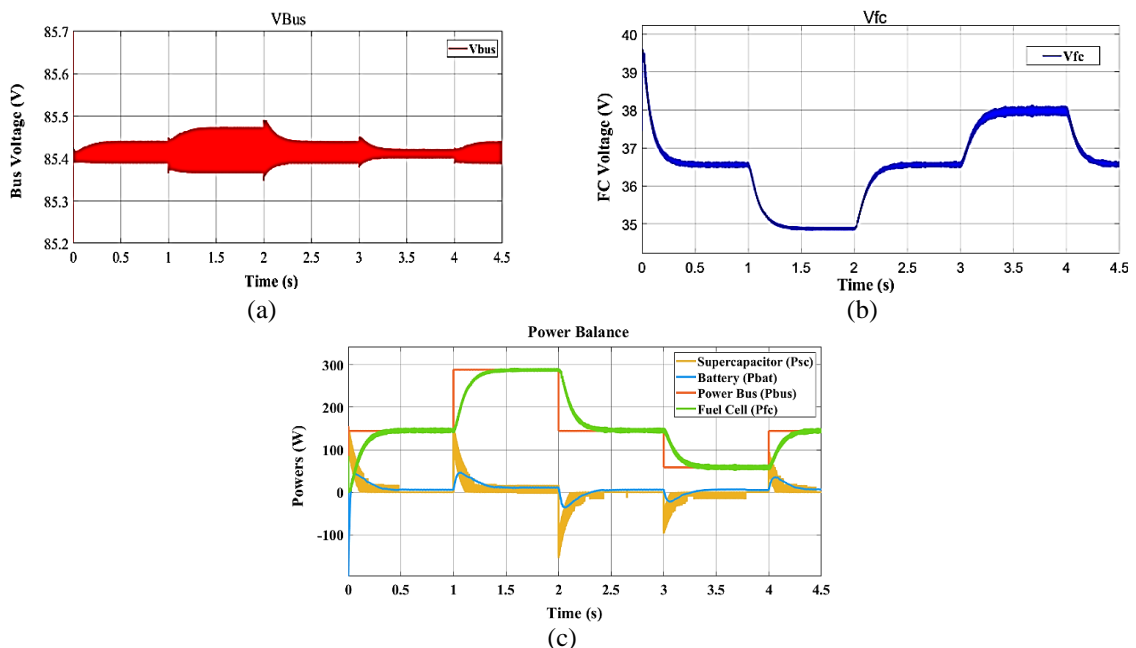


Figure 6. PEMFC based PEV simulation results: (a) bus voltage, (b) fuel cell output voltage, and (c) balancing (superposition) of all powers involved

5. EXPERIMENTATION AND VALIDATION

The presented work is based on a PEM fuel cell electronic replicator real time setup. A buck power electronic circuit realizes this emulator. The control strategy of this converter is controlled so that its behavior emulates a real PEM fuel cell. The usefulness of this test bench is the ability to perform the experiments without need to a real fuel cell. Such as, the input gas pressures, and temperature can be easily adjusted. The PEM fuel cell synoptic diagram associated with its boost DC-DC converter is shown in Figure 7, whereas Figure 8 shows the electronic schematic circuitry. The fuel cell electronic circuit consists of a main supply of 80 V providing energy to DC-DC buck converter through PID regulator using the fuel cell mathematical model. The real time experimental results are given in Figure 9 under a pure variable resistive load rating between 37 Ohms and 220 Ohms. Figure 9(a) shows respectively from top to bottom level, the output fuel cell voltage U_{fc} in Figure 9(a) curve (1), Q1 emitter output voltage in Figure 9(a) curve (2), the current through the coil L_1 in Figure 9(a) curve (3), and finally the Q1 control pulse signal issued from the dSPACE in Figure 9(a) curve (4). The operation of the PEMFC emulator under abrupt current load variation is illustrated in Figure 9b, where Figure 9(b) curve (5) is the emulator output voltage and Figure 9(b) curve (6) shows the output current. This fluctuation is typical and is in conformity with the PEMFC model.

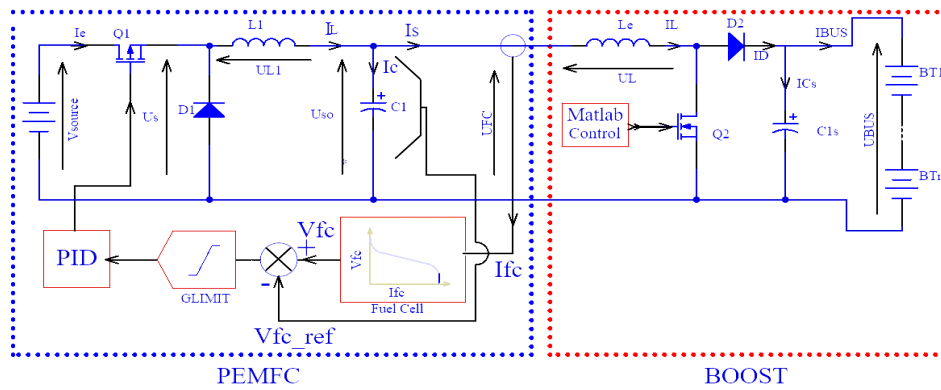


Figure 7. Schematic diagram of the PEM fuel cell emulator

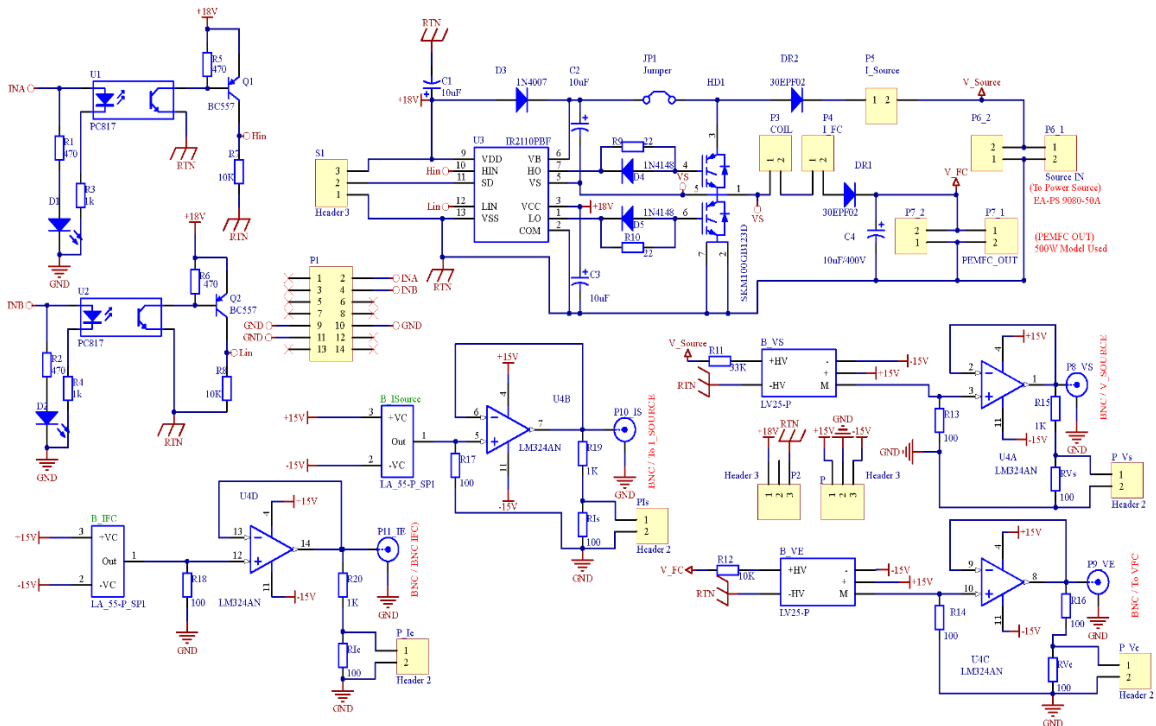


Figure 8. Electronic circuit of the PEMFC emulator

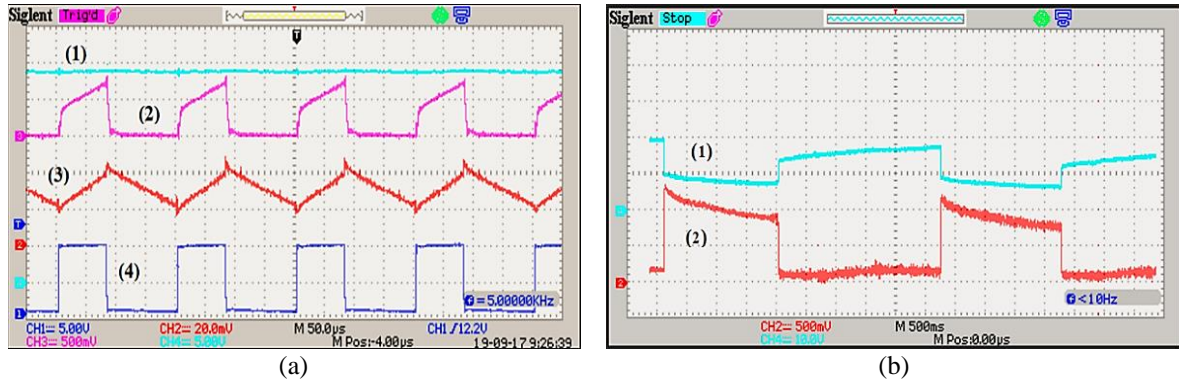


Figure 9. PEMFC real time experimental results: (a) (1) PEMFC output voltage, (2) Q1 emitter output voltage, (3) current through the coil L_1 , and (4) dSPACE 1103 Q1 control pulse signal; and (b) (1) emulator voltage output, and (2) emulator current output.

The resulted PEMFC output voltage supplies the boost stage, thus recharging the batteries and supercapacitor racks. Once the bus voltage V_{bus} produced, the used algorithm fixes three phases

- Phase 1: $V_{bus} < 84 V$. in this state the battery partially discharged are unable to provide alone the necessary output energy to the load, therefore the PEMFC provides all energy to supply the load and ensures the charging of the battery.
- Phase 2: $84 V < V_{bus} < 88 V$, the PEMFC still powering the whole of the system but, and the batteries are kept in a slow charging mode until they reach the full charge state.
- Phase 3: $V_{bus} > 88 V$: The Fuel cell switches off when the batteries reach its full charge state and ensure the supply of the load alone, until the bus level voltage drops down to 84 V.

The used DC-DC boost converter produces the Bus voltage is shown in Figure 10, is globally the same as the PEMFC emulator DC-DC buck converter enhanced with a performed adaptive algorithm. To achieve this, we need to monitor several currents and voltages such as the batteries current, the load current, the ultra-capacitor current, the bus voltage and finally the load voltage. The Buck/Boost converter works accordingly with voltage levels of the used sources: it switches on the buck stage for charging the supercapacitor when the available energy on the bus is in excess and switches on the boost stage when the energy stored in the supercapacitor is needed.

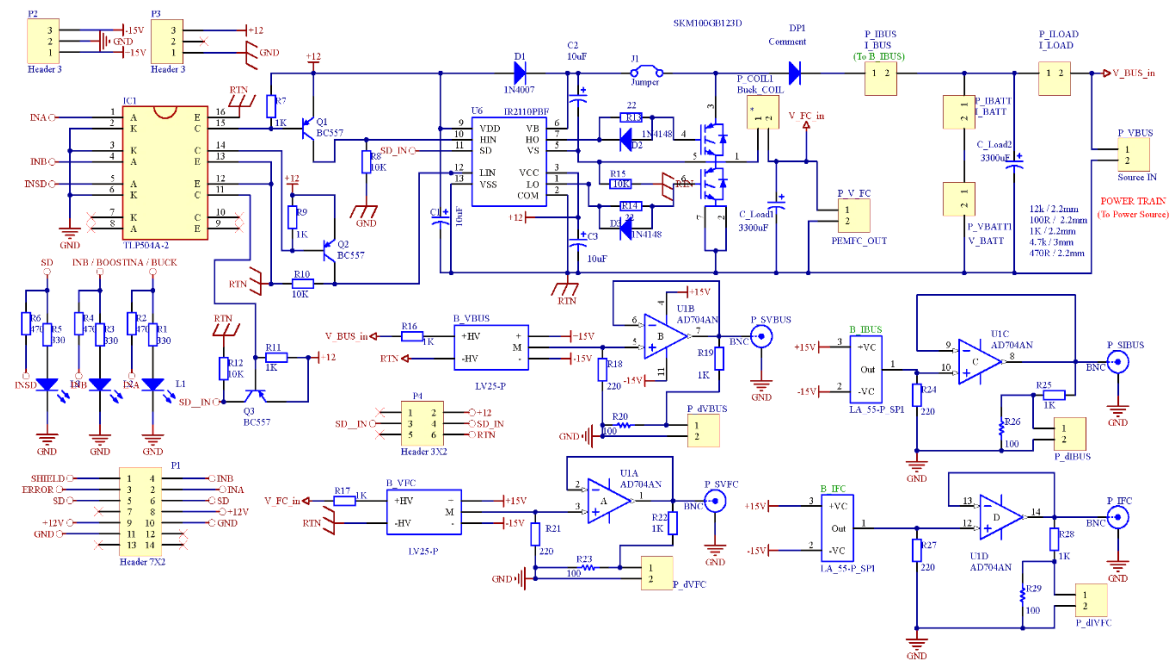


Figure 10. DC bus boost converter schematic

All the measured quantities are managed using MATLAB/Simulink toolbox through the dSPACE control desk interface to achieve the computation algorithm. The curves given in Figure 11 present the different results of the complete operational system. Where, Figure 11(a) shows the output fuel cell voltage feeding with the boost stage. Figure 11(b) shows the boost output voltage remaining between 76 V and 85 V, according to the behavioral cited in section 5. The Figures 11(c) and 11(d) show respectively the fuel cell and the load currents. Figure 11(e) shows the boost current feeding the load and the secondary sources both batteries and supercapacitor. Figure 11(f) shows the battery current in red and the supercapacitor current in green feeding with the bus voltage subsequently to the computation algorithm. Figure 12 shows the complete operational system built. The setup shown in Figure 12(a), gives the different subsystems including the dSPACE acquisition board, the converters, the load and finally the primary and secondary sources.

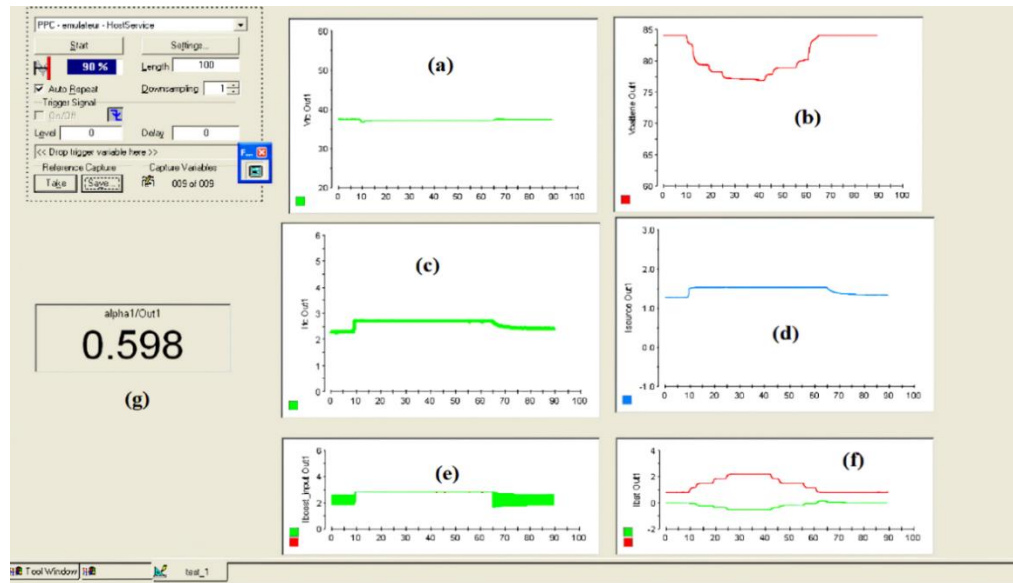


Figure 11. DC bus boost converter schematic; (a) the input source voltage, (b) the PEMFC output voltage, (c) the PEMFC emulator output current, (d) source current feeding with emulator, (e) C bus current, (f) battery current in red, and supercapacitor current in green, and (g) the applied duty cycle value computed by the designed PID

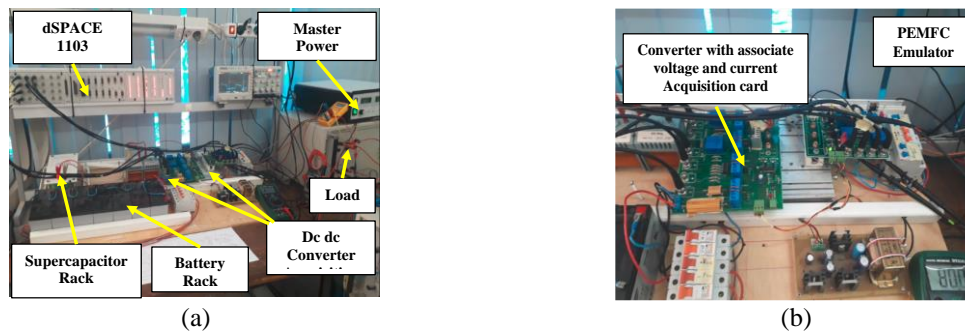


Figure 12. Experiment set up (a) global view on the whole system and (b) view on the acquisition card and the fuel cell emulator DC-DC converter

6. CONCLUSION

The PEM fuel cell emulator used to supply the EV power system has a real fuel cell behavior despite the several constraints imposed during the tests. Furthermore, the electronic topology and energy management system protocol (EMSP) recommended in this study can meet the energy requirements of the electric vehicle while adhering to the energy source exigencies, such as accommodating the dynamics of the PEMFC and handling the load needs thanks to the associated ESS. The results presented at the end of this work, demonstrate that the used configuration layout remains proficient, reliable, and straightforward, even with the existence of a further converter. Moreover, it delivers outstanding results with respect to power availability and autonomy.

ACKNOWLEDGEMENT

Authors thank the Ministry of Higher Education and Scientific Research for the financial of the equipment used in this work.




REFERENCES

- [1] V. Arora, T. Hodge, and T. Lidderdale, "Oil-Consumption-Weighted GDP : Description , Calculation , and Comparison," 2016.
- [2] M. H. Alzard *et al.*, "RoadCO 2 : A web-based tool for estimation of greenhouse gas emissions of road projects," in *2019 Advances in Science and Engineering Technology International Conferences (ASET)*, Mar. 2019, pp. 1–6. doi: 10.1109/ICASET.2019.8714341.
- [3] X. L. YUE and Q. X. GAO, "Contributions of natural systems and human activity to greenhouse gas emissions," *Advances in Climate Change Research*, vol. 9, no. 4, pp. 243–252, 2018, doi: 10.1016/j.accre.2018.12.003.
- [4] J. Van Mierlo, "The world electric vehicle journal, the open access journal for the e-mobility scene," *World Electric Vehicle Journal*, vol. 9, no. 1, 2018, doi: 10.3390/wevj9010001.
- [5] W. W. Hogan, "Electricity Market Design and Zero-Marginal Cost Generation," *Current Sustainable/Renewable Energy Reports*, vol. 9, no. 1, pp. 15–26, 2022, doi: 10.1007/s40518-021-00200-9.
- [6] A. Swarnkar and J. K. Maherchandani, "Performance Analysis of Hybrid Fuel Cell/Battery/Supercapacitor Electric Vehicle for Different Battery State of Charge Levels," *2018 International Conference on Recent Innovations in Electrical, Electronics and Communication Engineering, ICRIEECE 2018*, pp. 2306–2311, 2018, doi: 10.1109/ICRIECEE44171.2018.9008909.
- [7] S. A. R. Khan, Y. Zhang, A. Kumar, E. Zavadskas, and D. Streimikiene, "Measuring the impact of renewable energy, public health expenditure, logistics, and environmental performance on sustainable economic growth," *Sustainable Development*, vol. 28, no. 4, pp. 833–843, 2020, doi: 10.1002/sd.2034.
- [8] P. J. Young *et al.*, "Pre-industrial to end 21st century projections of tropospheric ozone from the Atmospheric Chemistry and Climate Model Intercomparison Project (ACCMIP)," *Atmospheric Chemistry and Physics*, vol. 13, no. 4, pp. 2063–2090, 2013, doi: 10.5194/acp-13-2063-2013.
- [9] P. Thounthong, B. Davat, and S. Raël, "Drive friendly," *IEEE Power and Energy Magazine*, vol. 6, no. 1, pp. 69–76, 2008, doi: 10.1109/MPAE.2008.4412942.
- [10] J. Bauman and M. Kazerani, "A comparative study of fuel-cell-battery, fuel-cell-ultracapacitor, and fuel-cell-battery-ultracapacitor vehicles," *IEEE Transactions on Vehicular Technology*, vol. 57, no. 2, pp. 760–769, 2008, doi: 10.1109/TVT.2007.906379.
- [11] C. Chavez-Baeza and C. Sheinbaum-Pardo, "Sustainable passenger road transport scenarios to reduce fuel consumption, air pollutants and GHG (greenhouse gas) emissions in the Mexico City Metropolitan Area," *Energy*, vol. 66, pp. 624–634, 2014, doi: 10.1016/j.energy.2013.12.047.
- [12] P. Garcia, L. M. Fernandez, C. A. Garcia, and F. Jurado, "Energy management system of fuel-cell-battery hybrid tramway," *IEEE Transactions on Industrial Electronics*, vol. 57, no. 12, pp. 4013–4023, 2010, doi: 10.1109/TIE.2009.2034173.
- [13] A. Khaligh and Z. Li, "Battery, ultracapacitor, fuel cell, and hybrid energy storage systems for electric, hybrid electric, fuel cell, and plug-in hybrid electric vehicles: State of the art," *IEEE Transactions on Vehicular Technology*, vol. 59, no. 6, pp. 2806–2814, 2010, doi: 10.1109/TVT.2010.2047877.
- [14] P. Jochem, S. Babrowski, and W. Fichtner, "Assessing CO2 emissions of electric vehicles in Germany in 2030," *Transportation Research Part A: Policy and Practice*, vol. 78, pp. 68–83, 2015, doi: 10.1016/j.tra.2015.05.007.
- [15] X. Lü *et al.*, "Energy management of hybrid electric vehicles: A review of energy optimization of fuel cell hybrid power system based on genetic algorithm," *Energy Conversion and Management*, vol. 205, 2020, doi: 10.1016/j.enconman.2020.112474.
- [16] B. Li *et al.*, "Modeling the impact of EVs in the Chinese power system: Pathways for implementing emissions reduction commitments in the power and transportation sectors," *Energy Policy*, vol. 149, 2021, doi: 10.1016/j.enpol.2020.111962.
- [17] A. Wang *et al.*, "Automated, electric, or both? Investigating the effects of transportation and technology scenarios on metropolitan greenhouse gas emissions," *Sustainable Cities and Society*, vol. 40, pp. 524–533, 2018, doi: 10.1016/j.scs.2018.05.004.
- [18] R. Tu, Y. (Jessie) Gai, B. Farooq, D. Posen, and M. Hatzopoulou, "Electric vehicle charging optimization to minimize marginal greenhouse gas emissions from power generation," *Applied Energy*, vol. 277, 2020, doi: 10.1016/j.apenergy.2020.115517.
- [19] Z. Li, A. Khajepour, and J. Song, "A comprehensive review of the key technologies for pure electric vehicles," *Energy*, vol. 182, pp. 824–839, 2019, doi: 10.1016/j.energy.2019.06.077.
- [20] E. Alpaslan *et al.*, "A review on fuel cell electric vehicle powertrain modeling and simulation," *Energy Sources, Part A: Recovery, Utilization and Environmental Effects*, 2021, doi: 10.1080/15567036.2021.1999347.
- [21] R. Moualek, N. Benyahia, A. Bousbaine, and N. Benamrouche, "Experimental Validation of Fuel Cell, Battery and Supercapacitor Energy Conversion System for Electric Vehicle Applications," pp. 239–245, 2021, doi: 10.1007/978-981-15-6595-3_31.
- [22] A. S. Samosir, M. Anwari, and A. H. M. Yatim, "A simple PEM fuel cell emulator using electrical circuit model," *2010 9th International Power and Energy Conference, IPEC 2010*, pp. 881–885, 2010, doi: 10.1109/IPECON.2010.5697090.
- [23] S. C. Ma, Y. Fan, J. F. Guo, J. H. Xu, and J. Zhu, "Analysing online behaviour to determine Chinese consumers' preferences for electric vehicles," *Journal of Cleaner Production*, vol. 229, pp. 244–255, 2019, doi: 10.1016/j.jclepro.2019.04.374.
- [24] P. Thounthong, S. Raël, and B. Davat, "Control algorithm of fuel cell and batteries for distributed generation system," *IEEE Transactions on Energy Conversion*, vol. 23, no. 1, pp. 148–155, 2008, doi: 10.1109/TEC.2006.888028.
- [25] A. Kolli, A. Gaillard, A. De Bernardinis, O. Bethoux, D. Hissel, and Z. Khatir, "A review on DC/DC converter architectures for power fuel cell applications," *Energy Conversion and Management*, vol. 105, pp. 716–730, 2015, doi: 10.1016/j.enconman.2015.07.060.
- [26] D. Y. Lee, A. Elgowainy, A. Kotz, R. Vijayagopal, and J. Marcinkoski, "Life-cycle implications of hydrogen fuel cell electric vehicle technology for medium- and heavy-duty trucks," *Journal of Power Sources*, vol. 393, pp. 217–229, 2018, doi: 10.1016/j.jpowsour.2018.05.012.
- [27] H. Wang, A. Gaillard, and D. Hissel, "A review of DC/DC converter-based electrochemical impedance spectroscopy for fuel cell electric vehicles," *Renewable Energy*, vol. 141, pp. 124–138, 2019, doi: 10.1016/j.renene.2019.03.130.
- [28] C. Y. Wong *et al.*, "Additives in proton exchange membranes for low- and high-temperature fuel cell applications: A review," *International Journal of Hydrogen Energy*, vol. 44, no. 12, pp. 6116–6135, 2019, doi: 10.1016/j.ijhydene.2019.01.084.
- [29] A. Anbarasu, T. Q. Dinh, and S. Sengupta, "Novel enhancement of energy management in fuel cell hybrid electric vehicle by an advanced dynamic model predictive control," *Energy Conversion and Management*, vol. 267, 2022, doi: 10.1016/j.enconman.2022.115883.
- [30] C. Si, X. D. Wang, W. M. Yan, and T. H. Wang, "A comprehensive review on measurement and correlation development of capillary pressure for two-phase modeling of proton exchange membrane fuel cells," *Journal of Chemistry*, vol. 2015, 2015, doi: 10.1155/2015/876821.
- [31] H. Chen, J. Chen, C. Wu, and H. Liu, "Fuzzy Logic Based Energy Management for Fuel Cell=Battery Hybrid Systems," *2018*




- European Control Conference, ECC 2018*, pp. 89–94, 2018, doi: 10.23919/ECC.2018.8550257.
- [32] H. Marzougui, A. Kadri, J. P. Martin, M. Amari, S. Pierfederici, and F. Bacha, "Implementation of energy management strategy of hybrid power source for electrical vehicle," *Energy Conversion and Management*, vol. 195, pp. 830–843, 2019, doi: 10.1016/j.enconman.2019.05.037.
- [33] H. Jiang, L. Xu, J. Li, Z. Hu, and M. Ouyang, "Energy management and component sizing for a fuel cell/battery/supercapacitor hybrid powertrain based on two-dimensional optimization algorithms," *Energy*, vol. 177, pp. 386–396, 2019, doi: 10.1016/j.energy.2019.04.110.
- [34] Amin, R. T. Bambang, A. S. Rohman, C. J. Dronkers, R. Ortega, and A. Sasongko, "Energy management of fuel cell/battery/supercapacitor hybrid power sources using model predictive control," *IEEE Transactions on Industrial Informatics*, vol. 10, no. 4, pp. 1992–2002, 2014, doi: 10.1109/TII.2014.2333873.
- [35] K. Chen, S. Laghrouche, and A. Djerdir, "Fuel cell health prognosis using Unscented Kalman Filter: Postal fuel cell electric vehicles case study," *International Journal of Hydrogen Energy*, vol. 44, no. 3, pp. 1930–1939, 2019, doi: 10.1016/j.ijhydene.2018.11.100.
- [36] A. L. Dicks and D. A. J. Rand, *Fuel Cell Systems Explained*. 2018. doi: 10.1002/9781118706992.
- [37] J. T. Pukrushpan, "Modeling and control of fuel cell systems and fuel processors," *Mechanical Engineering*, p. 133, 2003.
- [38] J. Xie, J. Ma, and K. Bai, "State-of-charge estimators considering temperature effect, hysteresis potential, and thermal evolution for LiFePO4 batteries," *International Journal of Energy Research*, vol. 42, no. 8, pp. 2710–2727, 2018, doi: 10.1002/er.4060.

BIOGRAPHIES OF AUTHORS






Riad Moualek    received his Master degree in electrical engineering from Mouloud Mammeri University, Tizi Ouzou, Algeria, in 2017. He is currently a PhD student at the same university. His research interests include energy management systems using fuel cells, batteries and supercapacitors, power electronics, embedded systems, renewable and sustainable energy resources. He can be contacted at email: rmoualekfr@yahoo.fr.






Nacereddine Benamrouche    received his PhD degree in electrical engineering from the University of Sheffield UK in 1990. He worked as a teaching assistant at The University of Leeds 1990-1991, and as head of department at Najran College of Technology, Saudi Arabia from 2000-2004. He is currently Professor at the Electrical Engineering and Computing Faculty, University of Tizi ousou, Algeria, where he occupied the chair of Vice chancellor for post graduate studies and research between 2007-2010. He is appointed as Laboratory Director of Advanced Technologies in Electrical Engineering since Mars 2011. His research interests include electrical machines and drives, control systems and renewable energy. He can be contacted at email: benamrouchen@yahoo.com.



Nabil Benyahia    Defended his Ph.D. in 2014 at University of Bejaia (Algeria) in optimization of electrical propulsion system: Application of Fuel cells and supercapacitors electric vehicle. Experimental works of his thesis was carried out at the CRTT of Saint-Nazaire and the Fuel Cell Laboratory (FC-LAB) at University of Belfort-Montbéliard. He has participated in several innovative projects in particular: Design of the newly initiated Rail Innovative Centre (RIC) based on power hardware in loop (P-HIL) demonstrator to meet the future propulsion systems for the rail at the university of Derby (UK), Design of an inverter based SiC component for high-speed magnet machines drives at ENSEM in Nancy, and Develop an experimental platform based on power hardware in the loop of PEM fuel cell and propeller for naval applications at NAVAL ACADEMY RESEARCH INSTITUE (Lanveoc). Currently, he is an assistant professor at ESME school (Paris). He can be contacted at email: nabil.benyahia@esme.fr.



Amar Bousbaine    Was born in Bouira in 1960. He received his Bsc, MSc and PhD respectively at the University of Tizi Ouzou in 1985 and at the University of Strathclyde in 1990 and at the University of Sheffield in 1995. He is currently reader in Electronics in the College of Engineering and Technology at the university of Derby, UK. He is also an active researcher in the field of power system for electric vehicles, renewable energy sources, hydrogen fuel cells and autonomous control for drives. He published over 70 papers in referred journal at: He can be contacted at email: a.bousbaine@derby.ac.uk.